https://doi.org/10.5194/egusphere-2024-2140
Preprint. Discussion started: 19 August 2024

The Impact of Scoria-Filled Aeration Trenches on the N-cycle and Greenhouse Gases Emissions from a Clayey Soil

Shahar Baram[1], Asher Bar-Tal[2], Anna Beriozkin[2], Roee Katzir[2], Alon Gal[1,3], David Russo[2]

[1] Institute of Soil, Water and Environmental Sciences, Agricultural Research Organization (ARO), Volcani Institute, Newe Ya'ar Research Center, Ramat Yishay, 30095, Israel.
[2] Institute of Soil, Water and Environmental Sciences, Agricultural Research Organization (ARO), Volcani Institute, 68 HaMacabim Rd. P.O Box 15159, Rishon Lezion 7505101, Israel.
[3] The Mina and Everard Goodman Faculty of Life Sciences, Bar-Ilan University, Ramat Gan, Ramat-Gan 52900, Israel.

Correspondence to: Shahar Baram (shaharb@volcani.agri.gov.il)

Abstract. Treated wastewater (TWW, i.e., treated effluents) is a growing water source. However, irrigation with TWW irrigation exacerbates oxygen deficiencies in the root zone, particularly in clayey soils. Coarse-textured filled trenches are used to ameliorate soil oxygen deficiencies in agriculture. This study aimed to investigate the impact of scoria-filled soil aeration trenches on nitrous oxide (N_2O) and carbon dioxide (CO_2) emissions from clayey soil irrigated with TWW. N_2O and CO_2 fluxes were measured in the field for three years, along with soil water content monitoring (10 and 35 cm depth) and porewater (30 cm depth) sampling. Irrigation and intense rain events led to transient (hours-long) near-saturation conditions in the clay soil. Concomitantly, the soil at the bottom of the trench remained saturated for prolonged periods, extending to days and even weeks. Nitrate was the dominant N-form and showed a seasonal trend with high concentrations (>50 mgL^{-1}) between June and October. N_2O fluxes were positively correlated with fertilizer applications, and fluxes from the trenches were higher throughout the year, with maximal differences during the winter. CO_2 fluxes were higher from the trenches during the fertigation seasons yet lower during the winter. Simulation results of N_2O fluxes showed higher fluctuation in the scoria-filled trenches following fertigation events. Further, it showed that filling the trench with finer medium, aimed to maximize the rate of water uptake by the trees' roots, increased the emissions maxima, dampening its minima. Overall, our study shows that aeration trenches may serve as N_2O hotspots and that, during winter, they might be counterproductive. Further study is needed to find the optimal filling material that would maximize aeration yet minimize water build-up at the trench bottom.

1. Introduction

The availability of treated wastewater (TWW), also known as treated effluents or reclaimed water, for agricultural purposes, is on the rise globally, correlating with the expanding global population (WWAP, 2017). In regions facing a scarcity of freshwater resources, the adoption of TWW for crop irrigation is rapidly increasing, underscoring its significance as a vital water resource (Assouline et al., 2015; Hamilton et al., 2007). However, research has demonstrated that prolonged utilization of TWW for irrigation results in notable deterioration of soil structure and hydraulic properties, primarily attributed to elevated exchangeable sodium percentages (ESP) (Assouline et al., 2015; Assouline and Narkis, 2013; Levy and Assouline, 2011; Stevens et al., 2003). Moreover, increased irrigation volumes are necessary to facilitate the leaching of salts present in TWW(Assouline and Narkis, 2013). These irrigation practices, in conjunction with the dissolved organic matter in TWW, exacerbate oxygen deficiency in agricultural soils, particularly in fine-textured soils with slow internal drainage (Assouline and Narkis, 2013; Ben-Noah and Friedman, 2016; Friedman and Naftaliev, 2012). In turn, such conditions may amplify denitrification processes, leading to increased N_2O emissions from the soils (Fillery, 1983).

N_2O represents both a significant degrader of stratospheric ozone (Ravishankara et al., 2009) and a potent greenhouse gas responsible for 6.24% of the total global radiative forcing (Butterbach-Bahl et al., 2013). Approximately 50% of annual N_2O emissions stem from human activities, with nitrogen additions in agriculture contributing around 70% of this total (Tian et al., 2020). These emissions primarily result from microbial processes of nitrification and denitrification in soils (Braker and

https://doi.org/10.5194/egusphere-2024-2140
Preprint. Discussion started: 19 August 2024

Conrad, 2011; Syakila and Kroeze, 2011). Key factors influencing N_2O emissions from agricultural lands include fertilizer application, soil temperature, and moisture content (Baram et al., 2018; Butterbach-Bahl et al., 2013; Syakila and Kroeze, 2011). Peak N_2O emissions typically occur when soil pore space is filled to 60-80% capacity with water (Davidson et al., 2000), although varying soil types may exhibit significant emissions under different moisture conditions (Butterbach-Bahl et al., 2013; Zechmeister-Boltenstern et al., 2007). In the last decade, research has also highlighted increased N_2O emissions from agricultural lands irrigated with treated wastewater (TWW) (González-Méndez et al., 2020; Shang et al., 2016; Xue et al., 2012; Zhu et al., 2023), emphasizing the augmented global warming potential associated with increased TWW usage for crop irrigation.

The practice of excavating trenches next to tree lines and subsequently filling them with coarse-textured materials (Ben-Noah and Friedman, 2018; Rubio-Asensio et al., 2018; Shamian et al., 2000; Tamir et al., 2022; Zipori et al., 2020) or profile mixing (Miyamoto and Nesbitt, 2011) represents a technique employed to ameliorate soil aeration challenges in planted orchards. The interface between the coarse-textured filling material and the underlying soil may form a hydrological barrier at the trench's bottom (Berezniak et al., 2018; Russo et al., 2020). This, in turn, may lead to water accumulation, impacting N transformations, volatilization, and soil respiration. Numerous models have been developed to simulate N_2O emissions from soils. Wherein these emissions primarily arise from nitrification and denitrification reactions and are influenced by various soil parameters including mineral N concentration, water-filled pore space (WFPS), temperature, pH, redox potential, and carbon (C) availability (Hénault et al., 2019; Rabot et al., 2015; Wu and Zhang, 2014). This study aimed to investigate the impact of soil aeration trenches on N_2O and CO_2 emission from clayey soil irrigated with TWW. Both field measurements and three-dimensional (3-D) simulations of flow and transport were utilized to study the intricate dynamics between water flow, N transport and transformations, and N_2O emissions.

2. Methods

2.1. Study area

A field study was conducted in a commercial 'Hass' avocado orchard (*Persea americana Mill.*) at Kibbutz Yasur (Latitude 32°53′46″ N and 35°10′22″ E), Israel. The orchard was established in 2009 and has been drip irrigated with secondary effluents (treated wastewater, TWW) ever since (see Supporting Information Table SI1). Detailed description of the orchard can be found in Nemera et al. (2023, 2020). In short, trees are planted 3.5m apart on ridges, with 6m between rows. The soil at the site is a Vertisol (58% clay dominated by montmorillonite, 19% silt, and 23% sand; Table SI2). The climate is Mediterranean, with a dry season (April – October) requiring irrigation, with rains during the winter (November – March).

In 2016, four random locations were selected, each containing 7 trees in three neighboring tree lines (Fig SI1). Trenches (0.3 m deep, 0.3 m wide, and 25 m long) were dug at these locations parallel to the tree line 0.3 m away from the tree trunks on both sides of the tree rows. The trenches were filled with a mixture of crushed volcanic Scoria and Tuff rocks (Tuff treatment). Drip laterals laid above the tuff trenches. From April through November, the orchard was fertigated every other day (control treatment), while the tuff treatment was fertigated seven times a week in the 2016, 2017, 2019, and 2020 growing seasons and ten times a day in the 2018 growing season. Both treatments were fertigated with an ammonium sulfate nitrate solution (NH_4:NO_3 = 3:1), maintaining 50 – 70 mg-N L^{-1} in the fertigation solution. The treatments received the same amount of water and N per week, with an annual N load of 350 kg-ha^{-1} and an irrigation depth of 850 mm. Out of the 350 kg-N, 50 kg-N came from the irrigation water (average N concentration was 6 mgL^{-1} (as ammonium-N)). Weekly water loads were based on reference ET_0, crop coefficient factors (K_c) with a 20 % leaching fraction. Precipitation depths in the winter of 2018 – 2019 and 2019 – 2020 were 859 and 739 mm, respectively.

2.2. N_2O and CO_2 sampling

https://doi.org/10.5194/egusphere-2024-2140
Preprint. Discussion started: 19 August 2024

From June 2018 through June 2020, N_2O and CO_2 fluxes were measured at mid-morning using accumulation static chambers that were installed at 8 random locations in the avocado orchard (Fig. SI1). At each location, a chamber base with a dripper at its center was inserted to a depth of 6-8 cm two weeks prior to the start of the sampling campaign and remained in the soil for the duration of the experiment (Fig. 1). The bases were made from opaque polyvinyl-chloride (PVC) rings, 10 cm high and 19 cm internal diameter (ID, surface area of 283.5 cm^2). The chambers were built from a 20 cm sewer PVC cup (volume of 3119 cm^3), equipped with a vent (3 mm Swagelok bulkhead union with a 12 cm long coiled copper tube, 1.5 mm i.d.), covered with a bubble reflective foil and a rubber skirt to ensure sealing with the base. Fluxes were measured in real-time by circulating the headspace in the static gas chamber via Teflon tubes into a Fourier-transform infrared spectrometer (FTIR; DX4015, Gasmet Technologies, Finland). During the enclosure period, N_2O and CO_2 concentrations were recorded every five seconds; each measuring point represents an average of 50 reads. Gas fluxes (q) [g cm^{-2} sec^{-1}] were calculated based on the linear slope, representing the increase in gas concentration throughout a 4 to 8 min enclosure time (Eq. 1). The Pearson's correlation coefficient (r^2) was calculated for the linearity of the slope, and readings were accepted when r^2 was >0.70.

$$q = \frac{dC_{gas}}{dt} * \frac{V_{chamber}}{A_{chamber}} * \frac{P}{RT} * M_w \quad (1)$$

where C_{gas} is the measured gas concentration [µL L^{-1}], t is the time [sec], $V_{chamber}$ [cm^3] and $A_{chamber}$ [cm^2] are the chamber volume and surface area respectively, P is the ambient pressure [atm], R is the gas law constant [0.08206 L atm mol^{-1} $^oK^{-1}$], T is the temperature [^{o}K], and M_w is the molecular weight of the gas [g mol^{-1}].

The trend of N_2O fluxes in the days following N applications (day after fertigation, DAF) was estimated in the field on three occasions (spring, summer, and fall). The collected data and the data reported in the literature for drip irrigation (Alsina et al., 2013; Baram et al., 2018; Garland et al., 2011; Kennedy et al., 2013; Schellenberg et al., 2012; Wolff et al., 2017; Zhang et al., 2016) were combined and used to create an exponential decay function for the N_2O flux in the DAF (Flux = $0.927e^{-0.607DAF}$) (Fig. SI2). Daily values for each chamber were obtained based on the decay function, linear interpolation, and numerical integration between sampling times. N_2O flux from the wetted zone around each dripper was calculated using equation 6 in Baram et al. (2018). Cumulative N_2O flux estimates were taken as the average of the cumulative fluxes of the 4 individual chambers, each (Parkin and Kaspar, 2006).

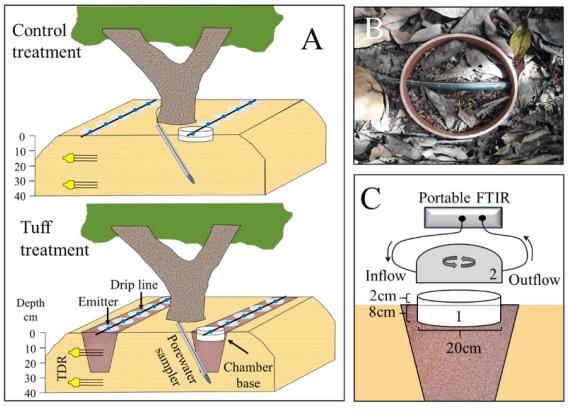

***Figure 1: (*A) Schematic illustration of the monitoring setup for each tree at the control (Ctrl) and Tuff treatments, which includes a porewater sampler at depth of 35 cm, two TRD probes at depths of 10 and 35 cm, and a static chamber used to measure gas fluxes. Drip laterals are located next to the tree lines or along the scoria-filled trenches, with light circles representing the wetting bulbs around the emitters. (B) Picture of a chamber base inside the trench. (D) The chamber base (1) and its cover (2) with the air inflow and outflow ports use to circulate the gas through a portable FTIR.**

2.3. Porewater sampling and soil monitoring

https://doi.org/10.5194/egusphere-2024-2140
Preprint. Discussion started: 19 August 2024

Porewater samplers (45 cm long SSAT, Irrometer Company, Inc. CA. USA) were installed at 30° to a depth of 30 – 35 cm under each static chamber base (Fig. 1). Porewater was sampled every 2 to 4 weeks throughout the same sampling period using a vacuum pump. All water samples were stored in polypropylene bottles and kept on ice until laboratory analysis. Water samples were analyzed for NO_3^- and NO_2^- concentrations with and without using vanadium (III) reduction (Doane and Horwáth, 2003), NH_4^+ concentrations as indophenol blue complex using salicylate (Kempers and Kok, 1989), and total N concentrations using the persulfate digestion method (APHA 4500-N C) (APHA, 1998).

At each of the eight monitoring sites, soil water content and temperature was measured at depths of 15 and 35 cm using True TDR sensors (Acclima, ID. USA) (Fig. 1). The sensors were connected to CR1000 (Campbell Scientific), and temperature and water content readings were taken every 15 min throughout the year.

2.4. Modelling water flow, nutrients fate, and N_2O emissions

2.4.1. The physical domain and its parametrization

The model used in this work was described in Russo et al. (2020), and Baram et al. (2022). In brief, a 3-D, spatially heterogeneous, variably saturated flow domain that extends over L_1=2 m, L_2=15 m, and L_3=10 m along the x_1, x_2, and x_3 Cartesian coordinate system, respectively, is considered here (where x_1 is directed downwards). The modeled subplot includes two adjacent tree rows on top of ridges, located 6 m apart, with four trees, located 3.5 m apart, along each row.

Following Russo et al. (2020), the van Genuchten (1980) (VG) five-parameter model (i.e., saturated conductivity, K_s, shape parameters, α and n, the saturated, θ_s, and residual, θ_r, values of water content, θ), was implemented for the local description of the constitutive relationships for unsaturated flow. Based on previous studies (e.g., Russo et al., 1997; Russo and Bouton, 1992), it was assumed that each of the VG parameters is a second-order stationary, statistically anisotropic, random space function characterized by a constant mean and a two-point covariance. Parameters of the latter, the variance and the correlation length scales, were adopted from Russo and Bouton (1992). Grain-size distribution data was obtained by the laser diffraction method (Eshel et al., 2004) from 0.3 m-segments of five soil cores extending to a depth of 1.2 m. The data was used to estimate the local-scale VG parameters by an optimization procedure. Mean values and coefficients of variation (CV) of the resultant VG parameters are given in Table 1 of Russo et al. (2020). The numerical grid used for the generation of the 3-D VG parameters field accounted for the application of water by the drip irrigation system and for the geometry of the ridges.

Both Tuff-filled aeration trenches and trenches filled with soil capable of maximizing the rate of water uptake by the trees' roots (K_s=15.52 m d^{-1}, α=0.94m^{-1}, and n=4) were modeled as described by Russo et al. (2020). Deterministic molecular diffusion coefficients ($D_{0)}$ for chloride (Cl^-), nitrate (NO_3^-) and ammonium (NH_4^+) in water, $D_0 = 5.4 \cdot 10^{-5}$ $m^2 d^{-1}$, dimensionless Henry's constant for N_2O, $K_H = 0.2$, and pore-scale dispersion tensor (with longitudinal dispersivity, $\lambda_L = 2 \times 10^{-3}$ m, and transverse dispersivity, $\lambda_T = 1 \times 10^{-4}$ m (Perkins and Johnston, 1963)), were considered in the simulations. First-order rate constants for nitrification and denitrification, K_1 and K_2, respectively, and a liquid-solid partitioning coefficient for ammonium, K_{d1}, were considered as depth-dependent, implementing values within the range suggested by (Lotse et al., 1992). Estimates of the root uptake coefficients for ammonium and nitrate, K_{u1} and K_{u2}, respectively, were calculated by extending the method of (Nye and Tinker, 1977); for more details, see (Russo et al., 2013). Root distribution data, adopted from (Salgado and Cautin, 2008), were employed in order to construct a time-invariant, normalized root depth-distribution function for the avocado trees.

2.4.2. Quantification of the flow and the transport

Considering water and N extraction by plant roots, water flow, and solute (NH_4^+, NO_3^-, and Cl^-) transport in the 3-D, unsaturated, spatially heterogeneous flow system were simulated employing numerical solutions of the 3-D Richards equation, and the 3-D single-region, advection-dispersion equation (ADE), respectively. The iterative procedure described in (Russo et

https://doi.org/10.5194/egusphere-2024-2140
Preprint. Discussion started: 19 August 2024

al., 2006) was employed in order to determine the size of the time-dependent ponding area that may develop around the drippers at the soil surface during an irrigation event. Furthermore, following Russo et al. (Russo et al., 2020), the sink term representing water uptake by the plant roots was modified to account for the effect of oxygen availability on water uptake. The maximization iterative (MI) approach proposed by Neuman et al. (Neuman et al., 1975) was adopted here in order to calculate water uptake by the plant roots and, concurrently, the actual transpiration rate, $\tau_a(t)$.

Following (Russo et al., 2013), the ADE was modified to account for N transformations and uptake by plants' roots in the soil-water-plant-atmosphere system. The competition between Cl^- and NO_3^- and its effect on the extraction of N by the plant roots, and the inhibition of nitrification induced by Cl^- were considered. For more details, see Russo and Kurtzman (Russo and Kurtzman, 2019). The uptake of NO_3^- and NH_4^+ by the plants' roots was also calculated by a MI approach described by Eq. 6 in (Russo et al., 2013).

Emissions of N_2O were calculated based on Hénault et al. (2005) and Hénault et al. (2019), accounting for nitrification and denitrification-driven emissions. N_2O flux during denitrification (N_2O_{denit}; mg-N m^{-2} d^{-1}) was calculated as a combination of the potential denitrification rate (D_P; mg-N m^{-2} d^{-1}) and response functions to several environmental factors (i.e., WFPS, assuming the WFPS parameter serves as a proxy of the oxygen availability for microorganisms, soil NO_3^- content, soil temperature), using a constant (r_{max}) representing the maximum ratio of N_2O to denitrified NO_3^- under anaerobic incubations (in this study r_{max} = 0.3) (Baram et al., 2022; Hénault et al., 2005). N_2O production during nitrification (mg-N m^{-2} d^{-1}) depended on the WFPS using a proportion constant (z) of nitrified nitrogen emitted as N_2O (in this study z = 0.006), r_{max}, and the actual areal nitrification rate (N_A; mg-N m^{-2} d^{-1}) (Baram et al., 2022; Hénault et al., 2005). Details of the flow and the transport equations and the numerical schemes employed to solve them are given elsewhere (Russo et al., 2013; Russo and Kurtzman, 2019).

Appropriate initial conditions for the present analyses were created by considering measured water content and solutes' concentrations profiles obtained prior to the irrigation season. For the flow, a second-type upper boundary condition was imposed on the top boundary (x_1 = 0) with flux that is determined by the drippers' discharge and by the time-dependent potential soil evaporation flux. A unit-head-gradient-boundary was specified at the bottom boundary (x_1=L1). For the transport, a first-type upper boundary condition was imposed on the top boundary with inlet concentrations corresponding to the irrigation water concentrations. A zero-gradient boundary was specified at the bottom boundary. No-flow conditions are assumed for the vertical boundaries located at x_2=0, x_2=L_2, x_3=0, and x_3=L_3.

2.4.3. Model implementation

Actual concentrations of NO_3^- and NH_4^+ in the irrigation water (including amounts added as fertilizers) and concentration of Cl^- in the irrigation water used in the field experiments were implemented in the simulations. Reference evapotranspiration $ET_0(t)$, was based on meteorological data collected at the site, using Penman-Monteith method. Potential evapotranspiration rates, $\varepsilon_{tp}(t) = \varepsilon_p(t) + \tau_p(t)$ (where ε: evaporation, τ - transpiration), were estimated from the $ET_0(t)$ data using the time-dependent crop coefficients used in the Yasur site. Assuming that the wetted soil surface area of the ridge is completely covered by the trees' canopy, a negligibly low soil evaporation rate was adopted for the surface area of the ridges, *i.e.*, $\tau_p(t) = \varepsilon\tau_p(t)$. For the soil surface area between the ridges outside the rooted zone, a negligibly small transpiration rate was assumed, *i.e.*, $\varepsilon_p(t)=\varepsilon\tau_p(t)$. Actual rates of water loss by evaporation, $\varepsilon_a(t)$, were implemented by an MI approach described in (Russo et al., 2006).

The chamber base was modeled as a cuboid whose axes coincide with the coordinates of the flow system as described in Baram et al. (2022). Unit-head-gradient was specified at the horizontal plane located at the bottom of the chamber (bottom boundary). For the transport, a first-type upper boundary condition was imposed on the top boundary with inlet concentrations corresponding to the irrigation water concentrations. No-flow (zero-gradient) was specified at the horizontal plane located at the top of the chamber and at the vertical planes, which coincide with the chamber's perimeter in the horizontal directions.

https://doi.org/10.5194/egusphere-2024-2140
Preprint. Discussion started: 19 August 2024

Starting at the beginning of the irrigation season (May 1st), flow and transport simulations, and N_2O emissions proceeded for an irrigation period of 180d. Actual concentrations of NO_3^- and NH_4^+ in the irrigation water (including amounts added as fertilizers) used in the field experiments were implemented in the simulations.

2.5. Statistics

Data was analyzed using JMP® Pro Statistical Software version 15.0 (SAS Institute Inc., USA). For each treatment, we used a t-test to analyze the effects of the tuff-filled trench on the measured and modeled parameters. The data met the assumption of homogeneity of variances. The impacts of soil-measured parameters on daily N_2O and CO_2 emissions were tested using Multiple Linear Regression (MLR) model. Presented data are means ± standard error (SE), with *p* values (*p*) representing the level of statistical significance.

3. Results

3.1. Soil water content

The volumetric water contents at depths of 10 and 35 cm in the Tuff and control treatments increased following irrigation and rain events (Fig. 2). Following rain events (November through March), and irrigation (April through October), the water content at 15 and 35 cm under the control treatments reached near saturation conditions (i.e., WC = 0.6, WFPS = 100%) which lasted for short periods (hours). The water contents in the clay at the tuff-clay interface (35 cm) and at 15 cm in the tuff-trench were impacted by the irrigation frequency and rain intensity. Intensive rains resulted in short periods (hours) of saturation in the trench (i.e., WC = 0.38), while the clay under the tuff-clay interface (35 cm) remained saturated (WC = 0.6, respectively) for days and even weeks (Fig 2A). Pulse irrigation (10 irrigations per day) kept the water content in the tuff-trench and in the clay under the tuff-clay interface at nearly constant values close to saturation (WC = 30±4% and 51±3%2, WFPS = 77±9% and 85±6%, respectively) (Fig 2B, C). Single irrigation per day led to fluctuation in the water content, reaching saturation for a short duration (hours), followed by quick drying of both the tuff in the trench and the clay under the tuff-clay interface (Fig 2).

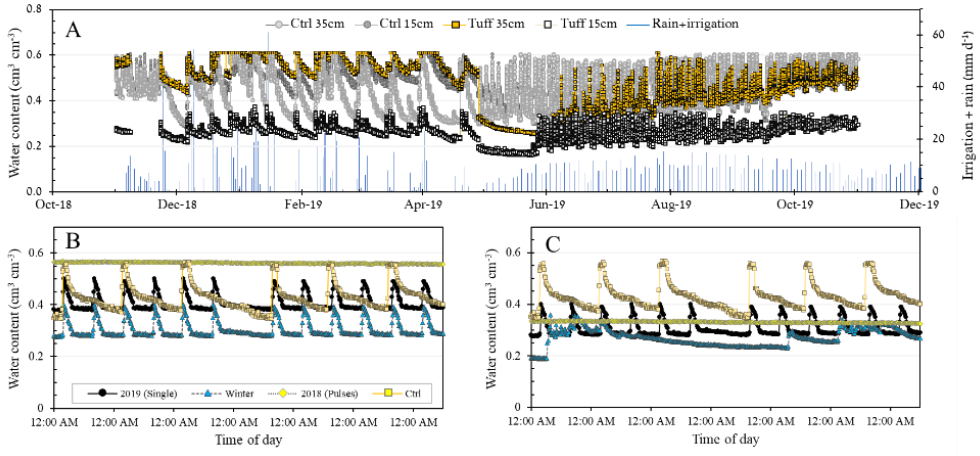

Figure 2: (A) Temporal dynamics of the volumetric water content measured by True TDR in the Ctrl and Tuff treatments throughout the year. (B) and (C) show daily dynamic from two consecutive weeks during the growing season where irrigation was applied in four pulses along the day (7 am to 2 pm) (June 2018 – circles) or once a day (7 am) (June 2019 – diamonds), and during the winter between two rain events (February 2019; winter – triangles). (B) shows data from the tuff-clay interface (depth of 30 – 35 cm) and the control (Ctrl), and (C) data from the shallow probes inside the trench (depth of 10 – 15 cm) and the control. Each data point represents an average reading of four sensors. Note that the saturation point of the Tuff is 39 – 40%, and that of the clay is 59 – 60%.

https://doi.org/10.5194/egusphere-2024-2140
Preprint. Discussion started: 19 August 2024

3.2. Porewater nitrogen concentrations

Over 930 porewater samples were collected between March 2018 and June 2020. Though ammonium was the dominant N form in the fertigation water (>40 mgL^{-1}), its concentrations in the soil porewater were low (< 2.5 mgL^{-1}) (Fig. 3A). Nitrite-N concentrations were normally low (<2.5 mgL^{-1}), except for five sampling dated during the fertigation season at which high concentrations (> 8 mgL^{-1}) where measured mainly under the Tuff treatment (Fig. 3B). Nitrate, was the dominant N form, and showed a seasonal trend with high concentrations (>50 mgL^{-1}) between June and October (Fig. 3C). Inspection of the daily trend during the fertigation season did not show a clear pattern, and the concentrations resembled the seasonal trend (fig. 3D).

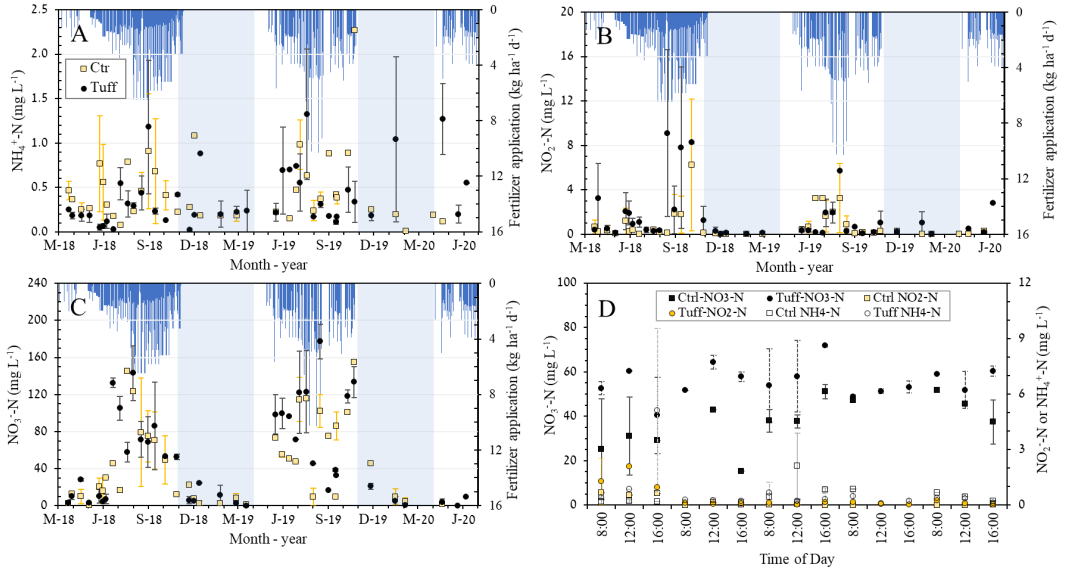

Figure 3: Seasonal dynamics of the (A) ammonium-N (NH_4^+-N) (B) nitrite-N (NO_2^--N), and (C) nitrate-N (NO_3^--N) concentrations in the porewater sampled from a depth of 35 cm under the Tuff and control (Ctrl) treatments. (D) Daily dynamics of the same N forms for five consecutive days in October 2018, where the Tuff treatment was irrigated daily and the Ctrl treatment once every other day. Presented are averages, with standard errors as vertical lines. In A, B, and C applied N loads (fertilizer plus TWW) are presented as vertical lines descending from the top, and shaded areas represent the wintertime

3.3. Nitrous oxide (N_2O) and carbon dioxide (CO_2) fluxes

Field measurements of N_2O fluxes from the soil surface indicated that the fluxes were lowest at 8 am, increased by 10 am, and hardly changed until 4 pm (Fig. SI3). Hence, fluxes were measured between 10 am and 2 pm and were thought to be representative of the daily flux. Throughout the monitoring period, N_2O fluxes were positively correlated with fertilizer applications. Fluxes measured during the fertigation period (April – October) in 2019 and 2020 were significantly higher than the fluxes measured in 2018 (Fig. 4A). A multi-parameter analysis (soil temperature, irrigation duration, water content, and nitrate nitrite and ammonium concentrations) could not elucidate the lower fluxes in 2018. During the two winters, average N_2O fluxes from the tuff treatment were higher (1.3 – 2.4 ng cm^{-2} min^{-1}) than the fluxes from the control (0.4 – 0.5 ng cm^{-2} min^{-1}), yet without a statistical significance (Table SI3). During the 2018 and 2020 fertigation seasons, the fluxes from the tuff were higher than the control (0.8 and 3.3 ng cm^{-2} min^{-1} vs. 0.5 and 2.1 ng cm^{-2} min^{-1}), while in 2019 it was higher in the control (3.5 vs. 4.6 ng cm^{-2} min^{-1}), all without a statistical significance (Table SI3). During the fertigation seasons, cumulative N_2O emissions from the Tuff treatment were higher than the control and amounted to 0.23% vs. 0.15%, 1.37% vs. 1.17%, and 1.53% vs. 1.51% in 2018, 2019, and 2020, of the applied N load, respectively (Table SI4). Cumulative N_2O emissions during the winter were about two times (1.7) higher in the Tuff treatment than in the control. In the winter of 2018-2019, it

https://doi.org/10.5194/egusphere-2024-2140
Preprint. Discussion started: 19 August 2024

accounted for 55% of annual emissions, while in 2019-2020, it accounted for 26% of annual emissions. Overall N_2O emissions in 2019 and 2020 were around 1.5% for both treatments and about 0.50% in 2018 (Table SI4).

Carbon dioxide (CO_2) fluxes from the soil surface showed a daily trend with a midday peak in the Tuff treatment, yet no trend in the control (Fig. SI3). Fluxes in the 2018 fertigation season were significantly lower than in 2019 and 2020 (Fig. 4B). In both treatments, emissions peaked from late spring (March) through late summer (September) and subsided in the fall. Cumulative emissions (ton CO_2 ha^{-1}) during the fertigation seasons were higher in the Tuff treatment than in the control (2018: 4.32 vs. 2.32; 2019: 13.4 vs. 8.25; 2020: 2.56 vs. 1.63) (Table SI5). In the winter of 2018-2019, emissions from the control treatment were significantly higher than the Tuff treatment, while in the winter of 2019-2020, they did not differ.

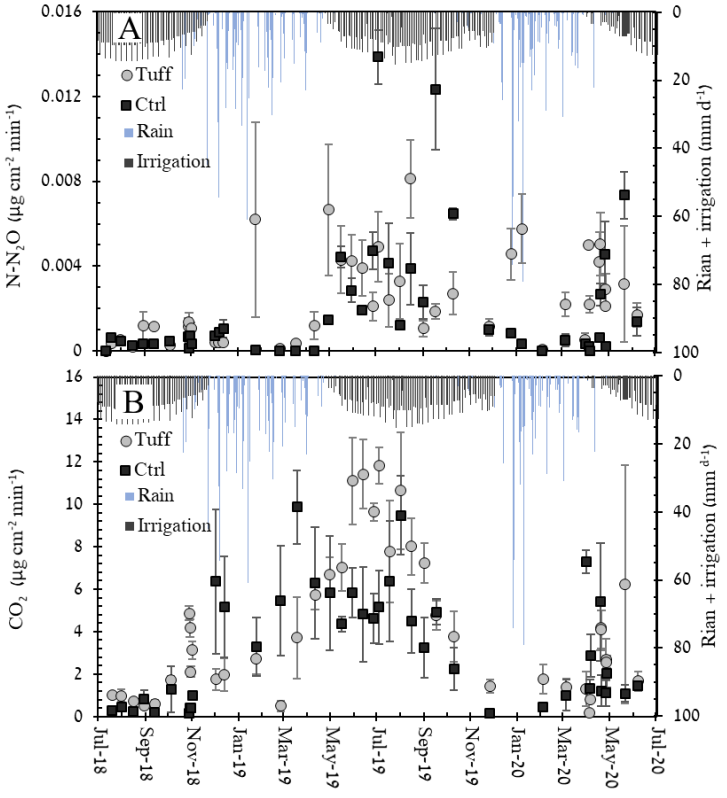

Figure 4: Seasonal dynamics of (A) nitrous oxide (N_2O-N) and (B) carbon dioxide (CO_2) emissions measured from June 2018 through June 2020. Presented are averages, with standard errors as vertical lines. Irrigations and rain are presented as black and blue vertical lines descending from the top.

3.4. Model results

Simulation results of N_2O fluxes showed higher fluctuation following fertigation events in the Tuff treatment relative to the natural clayey soil (Ctrl) (Fig. 5A). The use of a finer soil (media) aimed to maximize the rate of water uptake by the trees' roots from the aerating trench ("optimal"; i.e., SAop in Russo et al. (2020)) increased the emissions maxima, dampening its minima. Cumulative emissions following 60 days of fertigation showed a 4% decrease in the tuff and a 5% increase in the hydraulic optimal soil, relative to the clayey soil (Fig. 5B).

https://doi.org/10.5194/egusphere-2024-2140
Preprint. Discussion started: 19 August 2024

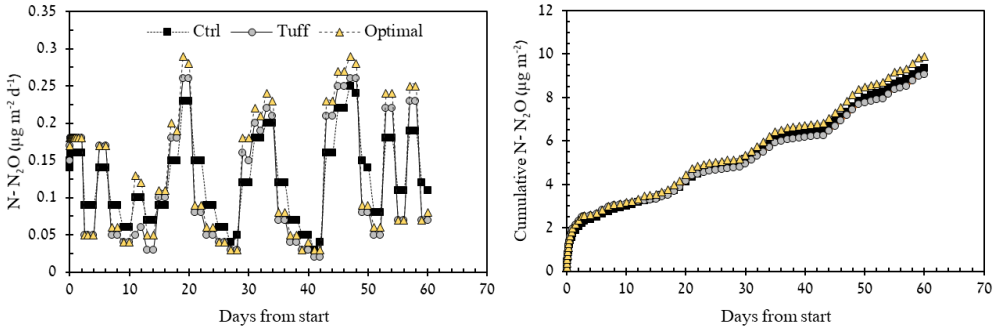

Figure 5: Simulation results of (A) temporal dynamics and (B) cumulative N-N_2O emissions during the fertigation season, and (C) changes over time in the ratio between the daily cumulative N-N_2O flux and the applied N load. Each point represents an average value of six emitters, three from each side of the tree. Ctrl. – the clayey soil at the site, Tuff – scoria-filled aeration trench, Optimal – soil aimed to maximize the rate of water uptake by the trees' roots from the aerating trench (i.e., SAop in Russo et al. (2020)).

4. Discussion

4.1. The effect of aeration trenches on N_2O emissions

In 2018, measured N_2O fluxes were very low (compared to 2019 and 2020), while CO_2 fluxes did not differ between the three years (Fig. 4). These similarities in CO_2 fluxes minimize the possibility of biased readings of N_2O fluxes due to technical errors in the measuring apparatus. It is possible, to some extent, that the placement of the chamber bases altered the microbial community structure and reduced the emissions. Nevertheless, such perturbation is not expected to last long, and the two-week gap between installation and measuring should have accounted for that (Clough et al., 2020). We do not know what drove the low emissions in 2018. As N_2O fluxes are renowned for their high temporal variability (Barton et al., 2015), the lower emissions of 2018 might have resulted from an inadequate sampling frequency. However, this is less likely as a similar frequency was used throughout the research period and post-fertilizer emission trends were observed in all three fertigation seasons (Fig. SI2).

As reported in the literature, N_2O emissions were positively correlated to N application. The measured fluxes in the 2019 and 2020 fertigation seasons were higher than what is commonly reported for drip irrigation (Alsina et al., 2013; Baram et al., 2018; Fentabil et al., 2016; Schellenberg et al., 2012). One possible explanation for the higher emissions measured in this work is the use of real-time *in-situ* measurements, which limits the closure period of the chamber, enabling high sensitivity (± 10 ppb), and minimizing biases associated with long closure periods (e.g., temperature, saturation, non-linearity) and sample handling (e.g., leakage). An additional factor may be the location of the chamber base (anchor) relative to the emitter. In this work, emitters were placed inside the chamber base, a practice that results in higher fluxes compared to the placement of the emitter outside the base (Baram et al., 2022). Baram et al. (2022) estimated that this bias can be minimized when accounting for the soils' capillary length. Hence, the use of a 20 cm i.d. chamber was sufficient for the Tuff treatment, yet a 40 cm i.d. chamber should have been used to represent the actual emission from the clayey soil. Nevertheless, it can be assumed that the measured fluxes represent the true differences between the two treatments, with a slight overestimation of the fluxes from the control.

Although the N-forms concentration in the irrigation water and the applied loads hardly differ between the years (Table SI3), emissions in 2018 were an order of magnitude lower at both treatments (Fig. 4A). In the Tuff treatment, the low emissions in 2018 might be an outcome of the pulse irrigation practiced that year. Pulse irrigation kept the WFPS at depths of 10 and 35 cm, at values close to saturation, with minor changes throughout the day, while in 2019 and 2020, the values fluctuated throughout the day, with short durations (hours) of near saturation values (Fig. 2). Under high WFPS (>80%), the solubility of N_2O in water, along with the short-term limits on diffusion, may reduce the accuracy of on-land measurements of

https://doi.org/10.5194/egusphere-2024-2140
Preprint. Discussion started: 19 August 2024

N_2O production (Smart and Peñuelas, 2005). Further, high WFPS promotes denitrification and might reduce N_2O emissions due to complete denitrification (Butterbach-Bahl et al., 2013; Wang et al., 2023).

Winter (2019 – 2020) N_2O emissions amounted to 34% and 24% of the total annual emissions (Table SI4). These values are on the lower end of the values (30% – 60%) reported for agricultural practices in Mediterranean climatic zones (Verhoeven et al., 2017). It is likely that the lower values reported here stem from the method used by us for upscaling the point measurements (i.e., chamber area) to the orchard scale (ha). In this work, we only accounted for the fluxes emitted from the wetted zones around the drip lines. During the fertigation period (spring – summer), the fluxes from the non-wetted zones were below detection, while in the winter, they were either below detection or very close to the detection limit. Integration of these low fluxes into the spatial budget would have increased the winter's contribution to the annual N_2O emission. Emissions during the winter were low due to low N concentrations in the topsoil profile (35 cm) (Fig. 3) and lower soil temperatures (Fig. SI4). Interestingly, in both winters, N_2O emissions from the Tuff treatment were 1.7 times higher than from the control. Probably, the increased emissions stem from the differences between the high hydraulic conductivity of the tuff-scoria gravel used to fill the trenches compared to the low conductivity of the clay soil. These differences lead to the accumulation of water at the trench's bottom (Fig. 2), and to the formation of hypoxic/ anaerobic conditions at the Tuff-clay interface which promotes denitrification.

The calculated emission factors for the 2019 and 2020 fertigation seasons (> 1.17%) (Table SI4) were higher than what is expected from drip irrigation in the Mediterranean climate (0.51%) (Cayuela et al., 2017; Sanz-Cobena et al., 2017). As with winter calculations, emissions were only calculated for the wetted zones around the drip lines, which accounted for 8.5% of the orchard's land surface area. Accordingly, the emission factors for the whole orchard were much lower and amounted to ~0.1%. These low values are promising as irrigation with TWW is thought to increase N_2O fluxes directly via degassing of dissolved N_2O, and indirectly by changing the physicochemical conditions in the soil and microbial activities (Thangarajan et al., 2012). Low dissolved oxygen concentrations in TWW (in this study, 4 – 2 mgL-1, data not presented) and its sodicity-induced structural damage (Assouline and Narkis, 2013; Levy and Assouline, 2011) promote the development of hypoxic conditions, favoring N_2O production and emissions (Saggar et al., 2004). Further, TWW irrigation may promote nitrite (NO_2^-) buildup in the soil (Master et al., 2003, 2004), as seen in this study (Fig. 2B). This N-species is intermediate in both nitrification (nitritation) and denitrification, and serves a substrate for N_2O production. Though high NO_2^- concentrations may inhibit denitrification in clayey soils (Master et al., 2003, 2004).

Overall, the reported N_2O fluxes show that the wetted zone around emitters on drip lines serves as hotspots for N_2O emission. Accordingly, the use of drip irrigation as a mitigation strategy for N_2O production (Cayuela et al., 2017), may be counterproductive when most of the field is wetted by the emitters' wetting bulbs (as commonly observed in field crops). In the case of aeration trenches, the very weak capillary forces of the scoria (tuff) filling material reduce the wetting bulb size, leading to a rapid decrease in its water content and hydraulic conductivity while concurrently creating conditions at the channels bed which favor N_2O production. Our simulation results show that filling the aeration trench with hydraulically optimal soil may increase water uptake but concomitantly increase the N_2O fluxes (Fig. 5). This soil, is characterized by a substantially lower conductance and substantially larger capillary forces, and substantially improve the soil aeration in the upper part of the soil profile, mainly during the rainfall seasons (Russo et al., 2020). These improved properties increase the total N_2O flux from the trench during the fertigation season (Figs. 5A and 5B). Mitigation of the irrigation frequency also impacts the N_2O fluxes. Pulse irrigation, maintains the water content in the trench, and at its bottom, at near saturation conditions (Fig. 2). This practice leads to a considerably shallower active root zone (Russo et al., 2020), enhancing the duration of denitrification favoring conditions, at the clay-tuff interface, and in the tuff.

4.2. The effect of aeration trenches on CO_2 emissions

https://doi.org/10.5194/egusphere-2024-2140
Preprint. Discussion started: 19 August 2024

Soil respiration (CO_2 fluxes) is the sum of heterotrophic (microbes, soil fauna) and autotrophic (root) respiration. Seasonal CO_2 emission was mainly driven by soil temperature, with high emission during the summer (soil temp 27°C), and low emissions during the winter (soil temp 12°C) (Fig. SI4). The soil remained moist year-round (WFPS >40%) and did not show a clear impact on soil respiration (Fig. 2). Differences between summer and winter emissions had a Q10 value of 3 – 6, which is higher than what is commonly reported for soils (Meyer et al., 2018). The differences were probably an outcome of increased root activity during the summer, as suggested by plant physiology and CO_2 assimilation values (Nemera et al., 2020). The diurnal cycle was not positively correlated to the soil temperature, which hardly changed throughout the day (<1°C) (Fig. SI4). It was lowest in the morning (5:00 – 6:00 am), peaked at midday (12:00 3:00 pm), subsiding in the evening. This daily trend is in good agreement with diurnal CO_2 assimilation, and assimilates transport to the root system (Nemera et al., 2020). A meta-analysis of agricultural soil respiration showed increased CO_2 fluxes following N addition (Lu et al., 2011; Zhou et al., 2014). On the seasonal scale (i.e., winter vs. fertigation) our observations agree with these findings (Table SI5). However, during the fertigation season, CO_2 fluxes did not differ much throughout the week, unlike the N_2O fluxes which were mainly regulated by N concentrations in the soil. This apparent discrepancy between the annual and weekly response of CO_2 emissions to N availability may be explained by the porewater nitrate concentration which hardly changed throughout the week (Fig. 3D).

The main purpose of aeration teaches is to promote root growth in a well aerated substrate, mitigating damages associated with hypoxic root zone. In this orchard, Nemera et al. (2020) showed higher sap flow, canopy conductance, and whole plant hydraulic conductance in the Tuff treatment during the fertigation season. Theses improved values could have enhanced the soil respiration, leading to higher CO_2 emissions from the Tuff treatment (Fig. 4B). In contrast, during the winter, CO_2 emissions were higher in the control treatment. This flip can be explained by (a) the low water holding capacity of the Tuff gravel, which hindered root uptake and respiration, and (b) flooding of the trenches following heavy rain events, that prevented root respiration and damaged the roots, especially close to the trenches bottom (Fig. 4A), (c) higher contribution of microbial respiration to the total soil respiration. Root respiration is clearly a combination of root activity and the activity of microorganisms in the rhizosphere, which can be distinguished using stable or radioactive isotope methods (Hanson et al., 2000; Pett-Ridge and Firestone, 2017). Although, stable or radioactive isotope methods were not used in this work, it is well established that the relative contribution of microbial respiration and root respiration to the total soil CO_2 flux (respiration) are driven by the physicochemical conditions in the soil and may fluctuate substantially (Hanson et al., 2000).

Annual carbon (C) assimilation by Avocado trees is assumed to range between 60 to 120 Mg ha^{-1} (Schaffer and Whiley, 2003). Based on our measurements C losses through CO_2 emission from the ridges amount to about 6 Mg ha^{-1} (representing 50% of the land area). Assuming the fluxes from the rest of the area were similar, annual CO_2 emission were 12 Mg ha^{-1}. In parallel, annual N_2O emissions equalled 0.35 kg ha^{-1} (assuming an emission factor of 0.1%), which equal 0.104 Mg CO_{2eq} (assuming 1 kg N_2O equals 298 kg CO_{2eq}), less than 1% of the net C assimilation. These values show the annual carbon sequestration potential of avocado orchards.

5. Conclusions

This work evaluated the impact of scoria filled aeration trenches (Tuff treatment) on N_2O emission, from a clayey soil irrigated with treated wastewater (TWW). Three years of field measurements in commercial avocado orchard showed that the tuff filled trenches increase the N_2O fluxes throughout the fertigation season and during the winter. Modeling efforts and field measurements show that most of the emissions come from the clay-tuff interface where high WFPS persists. High winter rains may flood the trenches, making them N_2O hotspots. Simulations show that filling the aeration trench with a hydraulically optimal soil may increase water uptake but concomitantly increase the N_2O fluxes. Balance between annual N_2O and CO_2 emissions and carbon assimilation by the trees, show that the orchard serves as a carbon sink. Accordingly, improved growth may balance the increased N_2O emissions from the trenches.

https://doi.org/10.5194/egusphere-2024-2140
Preprint. Discussion started: 19 August 2024

6. Author contribution

S. Baram and A. Bar-Tal supervised the project and acquired financial support. Baram designed the experiments, analyzed the data, and wrote the manuscript with contributions from all co-authors. D. Russo performed the detailed numerical simulations, A. Gal and R. Katzir collected the data in the field, and A. Beriozking conducted the chemical analysis.

7. Competing interests

The contact author has declared that none of the authors has any competing interests.

8. Acknowledgements

The study was funded by The Office of the Chief Scientist, Ministry of Agriculture and Rural Development, Israel, Grant No.20-03-0027. We thank the growers for allowing us to conduct the research at their farm.

9. References

Alsina, M. M., Fanton-Borges, A. C., and Smart, D. R.: Spatiotemporal variation of event related N_2O and CH_4 emissions during fertigation in a California almond orchard, Ecosphere, 4, art1, https://doi.org/10.1890/ES12-00236.1, 2013a.

APHA: Standard methods for the examination of water and wastewater, 20th ed., edited by: Clenceri, L. S., Greenberg, A. E., and Eaton, A. D., United Book Press, Baltimore, MD, 1998.

Assouline, S. and Narkis, K.: Effect of Long-Term Irrigation with Treated Wastewater on the Root Zone Environment, Vadose Zone Journal, 12, 0, https://doi.org/10.2136/vzj2012.0216, 2013.

Assouline, S., Russo, D., Silber, A., and Or, D.: Balancing water scarcity and quality for sustainable irrigated agriculture, Water Resour Res, 51, 3419–3436, https://doi.org/10.1002/2015WR017071, 2015.

Baram, S., Dabach, S., Jerszurki, D., Stockert, C. M., and Smart, D. R.: Upscaling point measurements of N_2O emissions into the orchard scale under drip and microsprinkler irrigation, Agric Ecosyst Environ, 265, 103–111, https://doi.org/10.1016/j.agee.2018.05.022, 2018a.

Baram, S., Dabach, S., Jerszurki, D., Stockert, C. M., and Smart, D. R.: Upscaling point measurements of N_2O emissions into the orchard scale under drip and microsprinkler irrigation, Agric Ecosyst Environ, 265, https://doi.org/10.1016/j.agee.2018.05.022, 2018c.

Baram, S., Bar-Tal, A., Gal, A., Friedman, S. P., and Russo, D.: The effect of static chamber base on N_2O flux in drip irrigation, Biogeosciences, 19, 3699–3711, https://doi.org/10.5194/bg-19-3699-2022, 2022.

Barton, L., Wolf, B., Rowlings, D., Scheer, C., Kiese, R., Grace, P., Stefanova, K., and Butterbach-Bahl, K.: Sampling frequency affects estimates of annual nitrous oxide fluxes, Sci Rep, 5, 15912, https://doi.org/10.1038/srep15912, 2015.

Ben-Noah, I. and Friedman, S. P.: Aeration of clayey soils by injecting air through subsurface drippers: Lysimetric and field experiments, Agric Water Manag, 176, 222–233, https://doi.org/10.1016/j.agwat.2016.06.015, 2016.

Ben-Noah, I. and Friedman, S. P.: Review and Evaluation of Root Respiration and of Natural and Agricultural Processes of Soil Aeration, Vadose Zone Journal, 17, 0, https://doi.org/10.2136/vzj2017.06.0119, 2018.

Berezniak, A., Ben-Gal, A., Mishael, Y., and Nachshon, U.: Manipulation of Soil Texture to Remove Salts from a Drip-Irrigated Root Zone, Vadose Zone Journal, 17, 1–11, https://doi.org/10.2136/vzj2017.01.0019, 2018.

Braker, G. and Conrad, R.: Diversity, Structure, and Size of N2O-Producing Microbial Communities in Soils—What Matters for Their Functioning?, Adv Appl Microbiol, 75, 33–70, https://doi.org/10.1016/B978-0-12-387046-9.00002-5, 2011.

Butterbach-Bahl, K., Baggs, E. M., Dannenmann, M., Kiese, R., and Zechmeister-Boltenstern, S.: Nitrous oxide emissions from soils: how well do we understand the processes and their controls?, Philos Trans R Soc Lond B Biol Sci, 368, 20130122, https://doi.org/10.1098/rstb.2013.0122, 2013.

Cayuela, M. L., Aguilera, E., Sanz-Cobena, A., Adams, D. C., Abalos, D., Barton, L., Ryals, R., Silver, W. L., Alfaro, M. A., Pappa, V. A., Smith, P., Garnier, J., Billen, G., Bouwman, L., Bondeau, A., and Lassaletta, L.: Direct nitrous oxide emissions in Mediterranean climate cropping systems: Emission factors based on a meta-analysis

https://doi.org/10.5194/egusphere-2024-2140
Preprint. Discussion started: 19 August 2024

of available measurement data, Agric Ecosyst Environ, 238, 25–35, https://doi.org/10.1016/j.agee.2016.10.006, 2017.

Clough, T. J., Rochette, P., Thomas, S. M., Pihlatie, M., Christiansen, J. R., and Thorman, R. E.: Global Research Alliance N2O chamber methodology guidelines: Design considerations, J Environ Qual, 49, 1081–1091, https://doi.org/https://doi.org/10.1002/jeq2.20117, 2020.

Davidson, E. A., Keller, M., Erickson, H. E., Verchot, L. V., and Veldkamp, E.: Testing a Conceptual Model of Soil Emissions of Nitrous and Nitric OxidesUsing two functions based on soil nitrogen availability and soil water content, the hole-in-the-pipe model characterizes a large fraction of the observed variation of nitric oxide an, Bioscience, 50, 667–680, https://doi.org/10.1641/0006-3568(2000)050[0667:tacmos]2.0.co;2, 2000.

Doane, T. A. and Horwáth, W. R.: Spectrophotometric Determination of Nitrate with a Single Reagent, Anal Lett, 36, 2713–2722, https://doi.org/10.1081/AL-120024647, 2003.

Eshel, G., Levy, G. J., Mingelgrin, U., and Singer, M. J.: Critical Evaluation of the Use of Laser Diffraction for Particle-Size Distribution Analysis, Soil Science Society of America Journal, 68, 736–743, https://doi.org/https://doi.org/10.2136/sssaj2004.7360, 2004.

Fentabil, M. M., Nichol, C. F., Jones, M. D., Neilsen, G. H., Neilsen, D., and Hannam, K. D.: Effect of drip irrigation frequency, nitrogen rate and mulching on nitrous oxide emissions in a semi-arid climate: An assessment across two years in an apple orchard, Agric Ecosyst Environ, 235, 242–252, 2016.

Fillery, I. R. P.: Biological denitrification, in: Gaseous loss of nitrogen from plant–soil systems, edited by: Frene, J. R. and Simpson, J. R., Martinus Nijhoff Publ., Dordrecht, the Netherlands., 33–64, 1983.

Friedman, S. P. and Naftaliev, B.: A survey of the aeration status of drip-irrigated orchards, Agric Water Manag, 115, 132–147, https://doi.org/10.1016/J.AGWAT.2012.08.015, 2012.

Garland, G. M., Suddick, E., Burger, M., Horwath, W. R., and Six, J.: Direct N 2O emissions following transition from conventional till to no-till in a cover cropped Mediterranean vineyard (Vitis vinifera), Agric Ecosyst Environ, 144, 423–428, https://doi.org/10.1016/j.agee.2011.11.001, 2011.

van Genuchten, M. Th.: A Closed-form Equation for Predicting the Hydraulic Conductivity of Unsaturated Soils, Soil Sci. Soc. Am. J, 44, 892–898, 1980.

González-Méndez, B., Ruiz-Suárez, L. G., and Siebe, C.: N2O emission factors from a wastewater irrigated land in a semiarid environment in Mexico, Science of The Total Environment, 709, 136177, https://doi.org/10.1016/j.scitotenv.2019.136177, 2020.

Hamilton, A. J., Stagnitti, F., Xiong, X., Kreidl, S. L., Benke, K. K., and Maher, P.: Wastewater irrigation: The state of play, Vadose Zone J., 6, 823–840, https://doi.org/doi:10.2136/vzj2007.0026, 2007.

Hanson, P. J., Edwards, N. T., Garten, C. T., and Andrews, J. A.: eparating root and soil microbial contributions to soil respiration: A review of methods and observations, Biogeochemistry, 48, 115–146, https://doi.org/10.1023/A:1006244819642, 2000.

Hénault, C., Bizouard, F., Laville, P., Gabrielle, B., Nicoullaud, B., Germon, J. C., and Cellier, P.: Predicting in situ soil N2O emission using NOE algorithm and soil database, Glob Chang Biol, 11, 115–127, https://doi.org/10.1111/j.1365-2486.2004.00879.x, 2005.

Hénault, C., Bourennane, H., Ayzac, A., Ratié, C., Saby, N. P. A., Cohan, J.-P., Eglin, T., and Gall, C. Le: Management of soil pH promotes nitrous oxide reduction and thus mitigates soil emissions of this greenhouse gas, Sci Rep, 9, 20182, https://doi.org/10.1038/s41598-019-56694-3, 2019.

Kempers, A. J. and Kok, C. J.: Re-examination of the determination of ammonium as the indophenol blue complex using salicylate, Anal Chim Acta, 221, 147–155, https://doi.org/10.1016/S0003-2670(00)81948-0, 1989.

Kennedy, T., Decock, C., and Six, J.: Assessing drivers of N_2O production in California tomato cropping systems., Sci Total Environ, 465, 36–47, https://doi.org/10.1016/j.scitotenv.2013.04.014, 2013.

Levy, G. J. and Assouline, S.: Physical aspects, in Use of Treated Waste Water in Agriculture: Impacts on the Soil Environment and Crops, chap. 9, edited by: Levy, G. J. et al., Wiley-Blackwell, Oxford, U.K., 306, 2011.

Lotse, E. G., Jabro, J. D., Simmons, K. E., and Baker, D. E.: Simulation of nitrogen dynamics and leaching from arable soils, J Contam Hydrol, 10, 183–196, https://doi.org/https://doi.org/10.1016/0169-7722(92)90060-R, 1992.

Lu, M., Zhou, X., Luo, Y., Yang, Y., Fang, C., Chen, J., and Li, B.: Minor stimulation of soil carbon storage by nitrogen addition: A meta-analysis, Agric Ecosyst Environ, 140, 234–244, https://doi.org/10.1016/j.agee.2010.12.010, 2011.

https://doi.org/10.5194/egusphere-2024-2140
Preprint. Discussion started: 19 August 2024

Master, Y., Laughlin, R. J., Shavit, U., Stevens, R. J., and Shaviv, A.: Gaseous Nitrogen Emissions and Mineral Nitrogen Transformations as Affected by Reclaimed Effluent Application, J Environ Qual, 32, 1204–1211, 2003.

Master, Y., Laughlin, R. J., Stevens, R. J., and ShavivA.: Nitrite Formation and Nitrous Oxide Emissions as Affected by Reclaimed Effluent Application, Journal of Environment Quality, 33, 852, 2004.

Meyer, N., Welp, G., and Amelung, W.: The Temperature Sensitivity (Q10) of Soil Respiration: Controlling Factors and Spatial Prediction at Regional Scale Based on Environmental Soil Classes, Global Biogeochem Cycles, 32, 306–323, https://doi.org/10.1002/2017GB005644, 2018.

Miyamoto, S. and Nesbitt, M.: Effectiveness of Soil Salinity Management Practices in Basin-irrigated Pecan Orchards, Horttechnology, 21, 569–576, https://doi.org/10.21273/HORTTECH.21.5.569, 2011.

Nemera, D. B., Bar-Tal, A., Levy, G. J., Lukyanov, V., Tarchitzky, J., Paudel, I., and Cohen, S.: Mitigating negative effects of long-term treated wastewater application via soil and irrigation manipulations: Sap flow and water relations of avocado trees (Persea americana Mill.), Agric Water Manag, 237, 106178, https://doi.org/10.1016/j.agwat.2020.106178, 2020.

Nemera, D. B., Yalin, D., Levy, G. J., Cohen, S., Shenker, M., Gothelf, R., Tarchitzky, J., and Bar-Tal, A.: Remediation and mitigation measures to counteract orchard soil degradation by treated wastewater irrigation, Soil Tillage Res, 234, 105846, https://doi.org/10.1016/j.still.2023.105846, 2023.

Neuman, S. P., Feddes, R. A., and Bresler, E.: Finite Element Analysis of Two-Dimensional Flow in Soils Considering Water Uptake by Roots: I. Theory, Soil Science Society of America Journal, 39, 224–230, https://doi.org/https://doi.org/10.2136/sssaj1975.03615995003900020007x, 1975.

Nye, P. and Tinker, P. B.: Solute Movement in the Soil-Root System, Blackwell Scientific Publications: Hoboken, NJ, USA, 342 pp., 1977.

Parkin, T. B. and Kaspar, T. C.: Nitrous oxide emissions from corn-soybean systems in the midwest., J Environ Qual, 35 4, 1496–1506, 2006.

Perkins, T. K. and Johnston, O. C.: A Review of Diffusion and Dispersion in Porous Media, Society of Petroleum Engineers Journal, 3, 70–84, https://doi.org/10.2118/480-PA, 1963.

Pett-Ridge, J. and Firestone, M. K.: Using stable isotopes to explore root-microbe-mineral interactions in soil, Rhizosphere, 3, 244–253, https://doi.org/10.1016/j.rhisph.2017.04.016, 2017.

Rabot, E., Cousin, I., and Hénault, C.: A modeling approach of the relationship between nitrous oxide fluxes from soils and the water-filled pore space, Biogeochemistry, 122, 395–408, https://doi.org/10.1007/s10533-014-0048-1, 2015.

Ravishankara, A. R., Daniel, J. S., and Portmann, R. W.: Nitrous oxide (N_2O): the dominant ozone-depleting substance emitted in the 21st century., Science, 326, 123–5, https://doi.org/10.1126/science.1176985, 2009.

Rubio-Asensio, J. S., Franch, V., López, F., Bonet, L., Buesa, I., and Intrigliolo, D. S.: Towards a near-soilless culture for woody perennial crops in open field conditions, Sci Hortic, 240, 460–467, https://doi.org/10.1016/j.scienta.2018.06.015, 2018.

Russo, D. and Bouton, M.: Statistical analysis of spatial variability in unsaturated flow parameters, Water Resour Res, 28, 1911–1925, https://doi.org/https://doi.org/10.1029/92WR00669, 1992.

Russo, D. and Kurtzman, D.: Using Desalinated Water for Irrigation: Its Effect on Field Scale Water Flow and Contaminant Transport under Cropped Conditions, Water (Basel), 11, 687, https://doi.org/https://doi.org/10.3390/w11040687, 2019.

Russo, D., Russo, I., and Laufer, A.: On the spatial variability of parameters of the unsaturated hydraulic conductivity, Water Resour Res, 33, 947–956, https://doi.org/https://doi.org/10.1029/96WR03947, 1997.

Russo, D., Zaidel, J., Fiori, A., and Laufer, A.: Numerical analysis of flow and transport from a multiple-source system in a partially saturated heterogeneous soil under cropped conditions, Water Resour Res, 42, https://doi.org/https://doi.org/10.1029/2006WR004923, 2006.

Russo, D., Laufer, A., Shapira, R. H., and Kurtzman, D.: Assessment of solute fluxes beneath an orchard irrigated with treated sewage water: A numerical study, Water Resour Res, 49, 657–674, https://doi.org/10.1002/wrcr.20085, 2013.

Russo, D., Laufer, A., and Bar-Tal, A.: Improving water uptake by trees planted on a clayey soil and irrigated with low-quality water by various management means: A numerical study, Agric Water Manag, 229, 105891, https://doi.org/https://doi.org/10.1016/j.agwat.2019.105891, 2020a.

https://doi.org/10.5194/egusphere-2024-2140
Preprint. Discussion started: 19 August 2024

Russo, D., Laufer, A., and Bar-Tal, A.: Improving water uptake by trees planted on a clayey soil and irrigated with low-quality water by various management means: A numerical study, Agric Water Manag, 229, 105891, https://doi.org/https://doi.org/10.1016/j.agwat.2019.105891, 2020b.

Salgado, E. and Cautin, R.: Avocado root distribution in fine and coarse-textured soils under drip and microsprinkler irrigation, Agric Water Manag, 95, 817–824, 2008.

Sanz-Cobena, A., Lassaletta, L., Aguilera, A., del Prado, A., Garnier, J., Billen, G., Iglesias, A., Sánchez, B., Guardia, G., Abalos, D., Plaza-Bonilla, D., Puigdueta-Bartolomé, I., Moral, R., Galán, E., Arriaga, H., Merino, P., Infante-Amate, J., Meijide, A., Pardo, G., Álvaro-Fuentes, J., Gilsanz, C., Báez, D., Doltra, J., González-Ubierna, S., Cayuela, M. L., Menéndez, S., Díaz-Pinés, E., Le-Noë, J., Quemada, M., Estellés, F., Calvet, S., van Grinsven, H. J. M., Westhoek, H., Sanz, M. J., Gimeno, B. S., Vallejo, A., and Smith, P.: Strategies for greenhouse gas emissions mitigation in Mediterranean agriculture: A review, Agriculture, Ecosystems and Environment Environment, 238, 5–24, 2017.

Schaffer, B. and Whiley, A. W.: Environmental regulation of photosynthesis in Avocado trees – a mini review, in: Proceedings V World Avocado Congress (Actas V Congreso Mundial del Aguacate), 335–342, 2003.

Schellenberg, D. L., Alsina, M. M., Muhammad, S., Stockert, C. M., Wolff, M. W., Sanden, B. L., Brown, P. H., and Smart, D. R.: Yield-scaled global warming potential from N_2O emissions and CH4 oxidation for almond (Prunus dulcis) irrigated with nitrogen fertilizers on arid land, Agric Ecosyst Environ, 155, 7–15, 2012a.

Shamian, S., Lowengart-Aycicegi, A., Antman, S., Aharon, M., Ran, Y., Rulf, R., Duvdevani, O., Aloni, N., and Sarig, T.: Increasing productivity and yields in nectarine orchard by tuff filled trenches - Shomera 98/99, Alon Hanotea, 54, 220–224, 2000.

Shang, F., Ren, S., Yang, P., Chi, Y., and Xue, Y.: Effects of Different Irrigation Water Types, N Fertilizer Types, and Soil Moisture Contents on N_2O Emissions and N Fertilizer Transformations in Soils, Water Air Soil Pollut, 227, 225, https://doi.org/10.1007/s11270-016-2920-1, 2016.

Smart, D. R. and Peñuelas, J.: Short-term CO_2 emissions from planted soil subject to elevated CO_2 and simulated precipitation, Applied Soil Ecology, 28, 247–257, https://doi.org/10.1016/j.apsoil.2004.07.011, 2005.

Stevens, D. P., McLughlin, M. J., and Smart, M. K.: Effects of long-term irrigation with reclaimed water on soils of the Northern Adelaide Plains, South Australia, Australian Journal of Soil Research, 41, 933–948, https://doi.org/10.1071/SR02049, 2003.

Syakila, A. and Kroeze, C.: The global nitrous oxide budget revisited, Greenhouse Gas Measurement and Management, 1, 17–26, https://doi.org/10.3763/ghgmm.2010.0007, 2011.

Tamir, G., Eli, D., Zilkah, S., Bar-Tal, A., and Dai, N.: Improving Rabbiteye Blueberry Performance in a Calcareous Soil by Growing Plants in Pits Filled with Low-$CaCO_3$ Growth Media, Agronomy, 12, 574, https://doi.org/10.3390/agronomy12030574, 2022.

Tian, H., Xu, R., Canadell, J. G., Thompson, R. L., Winiwarter, W., Suntharalingam, P., Davidson, E. A., Ciais, P., Jackson, R. B., Janssens-Maenhout, G., Prather, M. J., Regnier, P., Pan, N., Pan, S., Peters, G. P., Shi, H., Tubiello, F. N., Zaehle, S., Zhou, F., Arneth, A., Battaglia, G., Berthet, S., Bopp, L., Bouwman, A. F., Buitenhuis, E. T., Chang, J., Chipperfield, M. P., Dangal, S. R. S., Dlugokencky, E., Elkins, J. W., Eyre, B. D., Fu, B., Hall, B., Ito, A., Joos, F., Krummel, P. B., Landolfi, A., Laruelle, G. G., Lauerwald, R., Li, W., Lienert, S., Maavara, T., MacLeod, M., Millet, D. B., Olin, S., Patra, P. K., Prinn, R. G., Raymond, P. A., Ruiz, D. J., van der Werf, G. R., Vuichard, N., Wang, J., Weiss, R. F., Wells, K. C., Wilson, C., Yang, J., and Yao, Y.: A comprehensive quantification of global nitrous oxide sources and sinks, Nature, 586, 248–256, https://doi.org/10.1038/s41586-020-2780-0, 2020.

Verhoeven, Elizabeth., Pereira, Engil., Decock, Charlotte., Garland, Gina., Kennedy, T. ., Suddick, Emma., Horwath, William., and Six, Johan.: N_2O emissions from California farmlands: A review, California Agricalture, 71, 148–159, 2017.

Wang, H., Yan, Z., Ju, X., Song, X., Zhang, J., Li, S., and Zhu-Barker, X.: Quantifying nitrous oxide production rates from nitrification and denitrification under various moisture conditions in agricultural soils: Laboratory study and literature synthesis, Front Microbiol, 13, https://doi.org/10.3389/fmicb.2022.1110151, 2023.

Wolff, M. W., Hopmans, J. W., Stockert, C. M., Burger, Martin., Sanden, B. L., and Smart, D. R.: Effects of drip fertigation frequency and N-source on soil N_2O production in almonds, Agric Ecosyst Environ, 67–77, 2017.

Wu, X. and Zhang, A.: Comparison of three models for simulating N_2O emissions from paddy fields under water-saving irrigation, Atmos Environ, 98, 500–509, https://doi.org/https://doi.org/10.1016/j.atmosenv.2014.09.029, 2014.

https://doi.org/10.5194/egusphere-2024-2140
Preprint. Discussion started: 19 August 2024

WWAP ((United Nations World Water Assessment Programme): The United Nations World Water Development Report 2017, Wastewater: The Untapped Resource.Paris, UNESCO, 2017.

Xue, Y. D., Yang, P. L., Luo, Y. P., Li, Y. K., Ren, S. M., Su, Y. P., and Niu, Y. T.: Characteristics and Driven Factors of Nitrous Oxide and Carbon Dioxide Emissions in Soil Irrigated with Treated Wastewater, J Integr Agric, 11, 1354–1364, https://doi.org/10.1016/S2095-3119(12)60134-8, 2012.

Zechmeister-Boltenstern, S., Schaufler, G., and Kitzler, B.: NO_2, N_2O, CO_2 and CH_4 fluxes from soils under different land use: temperature sensitivity and effects of soil moisture, Geophys. Res. Abstr., 8, 7968, 2007.

Zhang, W., Zhou, G., Li, Q., Liao, N., Guo, H., Min, W., Ma, L., Ye, J., and Hou, Z.: Saline water irrigation stimulate N_2O emission from a drip-irrigated cotton field, Acta Agric Scand B Soil Plant Sci, 66, 141–152, https://doi.org/10.1080/09064710.2015.1084038, 2016.

Zhou, L., Zhou, X., Zhang, B., Lu, M., Luo, Y., Liu, L., and Li, B.: Different responses of soil respiration and its components to nitrogen addition among biomes: a meta-analysis, Glob Chang Biol, 20, 2332–2343, https://doi.org/10.1111/gcb.12490, 2014.

Zhu, Y., Wei, C., Chi, Y., and Yang, P.: The Influencing Mechanisms of Reclaimed Water on N_2O Production in a Multiyear Maize–Wheat Rotation, Agronomy, 13, 2393, https://doi.org/10.3390/agronomy13092393, 2023.

Zipori, I., Erel, R., Yermiyahu, U., Ben-Gal, A., and Dag, A.: Sustainable Management of Olive Orchard Nutrition: A Review, Agriculture, 10, 11, https://doi.org/10.3390/agriculture10010011, 2020.

10.